Contents lists available at ScienceDirect

Bioorganic & Medicinal Chemistry

journal homepage: www.elsevier.com/locate/bmc

Amphiphilic peptide-based MMP3 inhibitors for intra-articular treatment of knee OA

Cristian Guarise [a,*], Davide Ceradini [c], Martina Tessari [a], Mauro Pavan [a], Stefano Moro [b], Veronica Salmaso [b], Carlo Barbera [a], Riccardo Beninatto [a], Devis Galesso [a]

[a] Fidia Farmaceutici S.p.A., via Ponte della Fabbrica 3/A, 35031 Abano Terme (PD), Italy
[b] Molecular Modeling Section (MMS), Department of Pharmaceutical and Pharmacological Sciences, University of Padova, via Marzolo 5, 35131 Padova, Italy
[c] Latvian Institute of Organic Synthesis, Aizkraukles Iela 21, LV-1006 Riga, Latvia

ARTICLE INFO

ABSTRACT

Since 2007, Metalloproteases (MMPs) have been considered potential targets for treating osteoarthritis (OA), for which the primary pathogenic event is the extensive degeneration of articular cartilage. MMP3 is an enzyme critical for these degenerative changes. However, problems of selectivity, low bioavailability and poor metabolic profile during clinical trials of MMPs inhibitors (MMPIs) led to limited beneficial effect and thus did not justify further pursuit of the clinical studies. In a previous work, a new alkyl derivative of hyaluronic acid (HA), HYADD4®, previously approved as intra-articular treatment for knee OA, was studied *in vitro* and *in vivo* as MMP3I. Molecular simulation studies confirmed the interaction between the alkyl side chain of this HA derivative and the additional S1′ pocket of MMP3. However, the high MW and the polar HA backbone of HYADD4® imply a high desolvation energy cost, which can potentially decrease its inhibitory potency. In this study, a new class of MMP3Is based on a small peptide backbone (CGV) chemically derivatized with an alkyl chain was developed through interactive cycles of design, synthesis and screening, accompanied by computational evaluation and optimization. Two MMP3Is, e(I) and l(II), were selected because of their effective inhibitory activity (3.2 and 10.2 μM, respectively) and water solubility. Both MMPIs showed a broad range of inhibitory effects against almost all the MMPs tested. In an *in vitro* model of inflammatory OA, e(I) was the most effective MMPI: at the concentration of 93 μM, it reversed inflammatory outcomes. Moreover, because of its amphiphilic structure, the e(I) MMPI promoted stable micellar formulation at concentrations higher than 0.2 mg/mL in water. The findings were confirmed by TEM and Nile red staining analysis. Based on these results, the e(I) MMPI can be considered a good candidate for the intra-articular treatment of OA, and the micellar formulation of this peptide in an aqueous buffer can potentially increase the bioavailability and, thus, the efficacy of the MMPIs.

1. Introduction

Matrix metalloproteinases (MMPs) are zinc-dependent endopeptidases that constitute a family with 24 members in mammals.[1] Because of their ability to degrade the extracellular matrix (ECM) and to process a large number of bioactive molecules, MMPs play significant roles in many physiological situations, such as bone remodelling,[2] tissue homeostasis,[3] host defence[4] and tissue repair.[5] MMPs display formidable proteolytic activity, and MMP deregulation can lead to different diseases with focal tissue destruction (*e.g.,* rheumatoid arthritis,[6] osteoarthritis,[7] chronic cutaneous ulceration,[8] neurodegenerative disorders,[9] and cancer progression).[10]

The development of MMP inhibitors (MMPIs) has therefore been an attractive strategy for therapeutic intervention. Thus far, only one MMPI has been successfully launched (i.e., Periostat® by CollaGenex Pharmaceutical Inc., for the treatment of periodontal disease[11]), despite >50 MMPIs being investigated in clinical trials. Valuable lessons were learned from prior clinical trial failures, including the need for selective and metabolically stable inhibitors with high bioavailability. However, as a better understanding of MMP biology and inhibitor pharmacokinetic properties emerged, it became clear that initial MMP inhibitor clinical trials were held prematurely.

Since 2007, MMPs have been considered potential targets for treating osteoarthritis (OA).[12] MMPs are physiologically downregulated by

---

tissue inhibitors of metalloproteases (TIMPs). The modification of endogenous-like inhibitors (TIMP analogues) has been explored in attempts to design selective MMPIs, but an additional concern has been raised about their ability to penetrate cartilage, which is needed for OA application.[13,14] Based on the literature, MMP3 (stromelysin 1) can be considered a promising target in OA progression: it plays an important role in the MMP cascade owing to its ability to degrade various components of cartilage, such as gelatine, aggrecan, and collagen types III, IV, IX, and X, and it activates pro-MMP 1, 7, 8, 9, and 13.[15]

In our previous work, new alkyl derivatives of hyaluronic acid (HA), named HYADD4®, previously approved as an intra-articular treatment of knee OA, were selected as the strongest MMPIs in a series of glycosaminoglycans and derivatives. Molecular modelling studies suggested an interaction between the alkyl side chain of the HA derivative and the additional S1′ pocket of the MMPs[16]; however, the high MW of the polar HA backbone of HYADD4® implies a high desolvation energy cost, which can potentially decrease the inhibitor potency.

The aim of this work is to design a new class of MMP3 inhibitors, maintaining the alkyl side chain but substituting the HA backbone with a small peptide backbone to increase their affinity and to decrease the desolvation energy cost. To this end, a peptide sequence with micromolar MMPI, previously described in literature by Hanglow et al.[17] and Steele et al.[18], was used as a template for the *in silico* design of two series of peptides, which were synthesized and tested with a specific MMP3 assay. The inhibitors were developed through interactive cycles of design, synthesis, screening and computational evaluation and optimization. MMP3 inhibitors were selected as hit compounds and further tested for selectivity against ten different human MMPs, while its cytotoxicity was evaluated *in vitro*. Finally, the inhibitor efficacy was assessed by means of an *ex vivo* assay, in which the collagen released from inflamed biopsy samples of bovine cartilage was quantified after 3 weeks of incubation with the MMPIs and compared to untreated control samples.

2. Materials

Enzo Life Sciences, Inc. (US) supplied the Fluorimetric MMP Inhibitor Profiling Kit. Biocolor Ltd. (UK) supplied the Sircol collagen assay. All other reagents were supplied by Sigma and used without further purification.

2.1. Molecular modelling: Molecular docking

The X-ray crystallographic structure of MMP3, bound to the inhibitor RO–26–2812, was retrieved from the Protein Data Bank (PDB code: 1C3I[18]). The protein structure was prepared employing the Structure Preparation and Protonate 3D[19] tools of the Molecular Operating Environment (MOE) software suite[20]. The novel peptide-based compounds were built in place using the experimental structure of RO-26–2812 as a template, and then minimized with the Amber12EHT Force Field. The electrostatic and van der Waals components of the peptide-protein interaction energy were computed. MOE software was used for the entire modelling process[21].

2.2. Synthesis of the peptide-based MMPIs: Series I

Solid-phase peptide synthesis (SPPS) of this series of peptides was performed on Wang resin (150 mg; 0.17 mmol; 1 Eq) at RT in a cylindrical vessel (Fig. 1). Five equivalents of the first Fmoc-AA-OH (AA: generic amino acid) was dissolved in 2 mL of DMF with 5 Eq of *N*'-diisopropylcarbodiimide (DIC); then, 0.2 Eq of 4-dimethylaminopyridine (DMAP) was added, and the vessel was shaken for 2 h. After washing the resin with DMF/DCM 1:1 (5 × 2 mL), acetic anhydride (8 Eq) and *N*-methylmorpholine (8 Eq) in 1 mL of dichloromethane (DCM) were added, and the vessel was shaken for another hour. Fmoc removal was performed by treating the resin twice with 2 mL of DMF:piperidine 8:2

for 15 min each time. The subsequent steps were performed following standard Fmoc synthesis procedures until the last AA was generated. Each coupling was repeated twice using 5 Eq of benzotriazol-1-yl-oxytri (pyrrolidino)-phosphonium hexafluorophosphate (PyBOP) as the coupling reagent and 8 Eq of *N*-diisopropylethylamine (DIPEA) as the base (duration of each coupling: 1.5 h). Finally, Fmoc was removed, and 5 Eq of acyl fluoride in 2 mL of DCM and 10 Eq of DIPEA were added to the resin and shaken for 2 h. After washing with DMF:DCM 1:1 (5 × 2 mL), the peptide was cleaved from the resin with 2 mL of a solution consisting of trifluoroacetic acid (TFA) 88%/H$_2$O 5%/phenol 5% and TIPS 2%, precipitated in cold diethyl ether and purified to the greatest extent possible by means of semipreparative HPLC. Each MMPI was characterized by HPLC-MS analysis (see Supporting Information for details).

2.3. Synthesis of the peptide-based MMPIs: Series II

The SPPS of this series of peptides was performed on Rink resin (200 mg; 0.10 mmol; 1 Eq) as solid phase, at RT, in a cylindrical vessel (Fig. 1). After Fmoc removal (treating the resin with 2 mL of DMF: piperidine 8:2 twice for 15 min each time), the starting Fmoc-Asp(OAll)–OH was coupled by adding 5 Eq of Fmoc-AA-OH (AA: generic amino acid), 5 Eq of PyBOP and 8 Eq of DIPEA in 2 mL of DMF in a cylindrical vessel, and shaken for 2 h. After Fmoc deprotection, as previously described, the subsequent steps were performed following standard Fmoc synthesis until the last AA was generated (without *N*-terminal Fmoc group removal). After resin washing with DMF:NMP 1:1 (5 × 2 mL), 3 Eq of Pd(PPh$_3$)$_4$ and 7 Eq of PhSiH$_3$, as the catalyst system in 2 mL of DCM, were added. After shaking the vessel for 2 h in a nitrogen atmosphere, washing was performed first with DCM and DMF, subsequently with 5% DIPEA in DCM and finally with 5% DIPEA in DMF. Then, the reagents and solvents were added to the resin following a precise order: 0.8 mL of DMF, 8 Eq of DIPEA and 5 Eq of PyBOP in 1.5 mL of DCM. The vessel was shaken for 1.5 h, and then, the resin was washed as previously described. Five equivalents of alkyl amine was dissolved in 1.5 mL of DMF with 8 Eq of DIPEA, added to the resin, and shaken for 2 h, followed by resin washing with DMF/DCM 1:1 (5 × 2 mL). After Fmoc deprotection (and eventual acetylation), the peptide was cleaved from the resin with 2 mL of a solution consisting of TFA 88%/H$_2$O 5%/phenol 5% and TIPS 2%, precipitated in cold diethyl ether and purified to the greatest extent possible by means of semipreparative HPLC. Each MMPI was characterized by HPLC-MS analysis (see Supporting Information for details).

2.4. Screening of MMPIs on human MMPs

The inhibitory potencies of the peptide-based MMPIs were tested on the catalytic subunits of human MMPs using a fluorometric MMP inhibitor profiling kit (BML-AK016). The MMPIs were dissolved in DMSO at a concentration of 3 mg/mL. Next, each solution was diluted in DMSO or PBS to the desired concentration. MMPIs were screened at 0.030 mg/mL, 0.015 mg/mL and 0.0075 mg/mL using the same substrate concentration (4.0 μM). Initial rates (RFU/s) in the presence of each MMPI were normalized to the initial rate in the presence of PBS buffer (pH = 7). All samples were tested in three replicates. The IC$_{50}$ value was determined to fit with a sigmoidal plot of the normalized MMP activity *vs.* the MMPI concentration.

2.5. Cytotoxicity assay

The biocompatibility of the tested compounds (MMPIs: e(I) and l(II)) was evaluated by means of a quantitative analysis according to the ISO 10993–5:2009 international standard for the biological evaluation of medical devices. All the samples tested were sterilized by filtration at 0.2 μm. The cytotoxicity study was performed using BALB/3T3 clone A31 mouse fibroblasts (ATCC® CCL-163), as previously described[22]. All
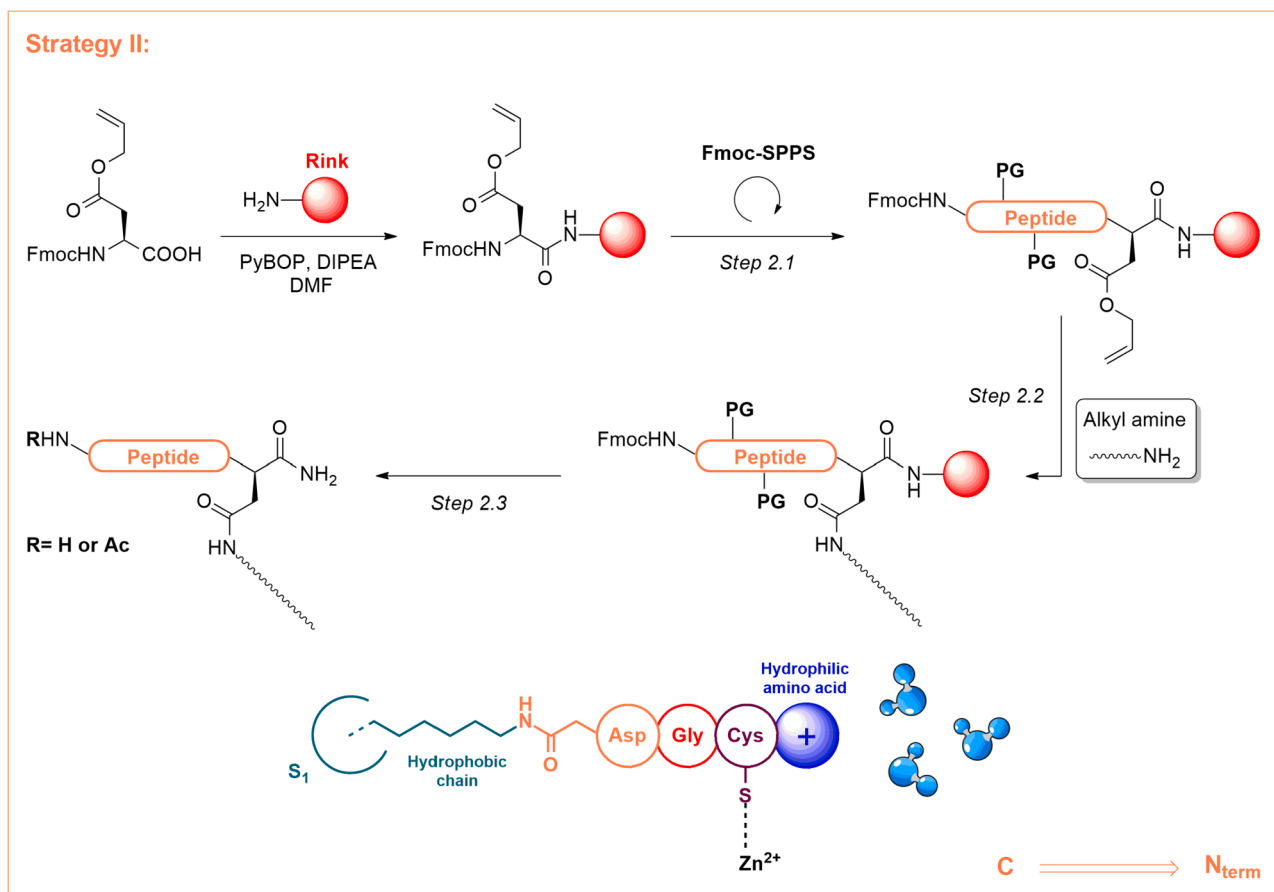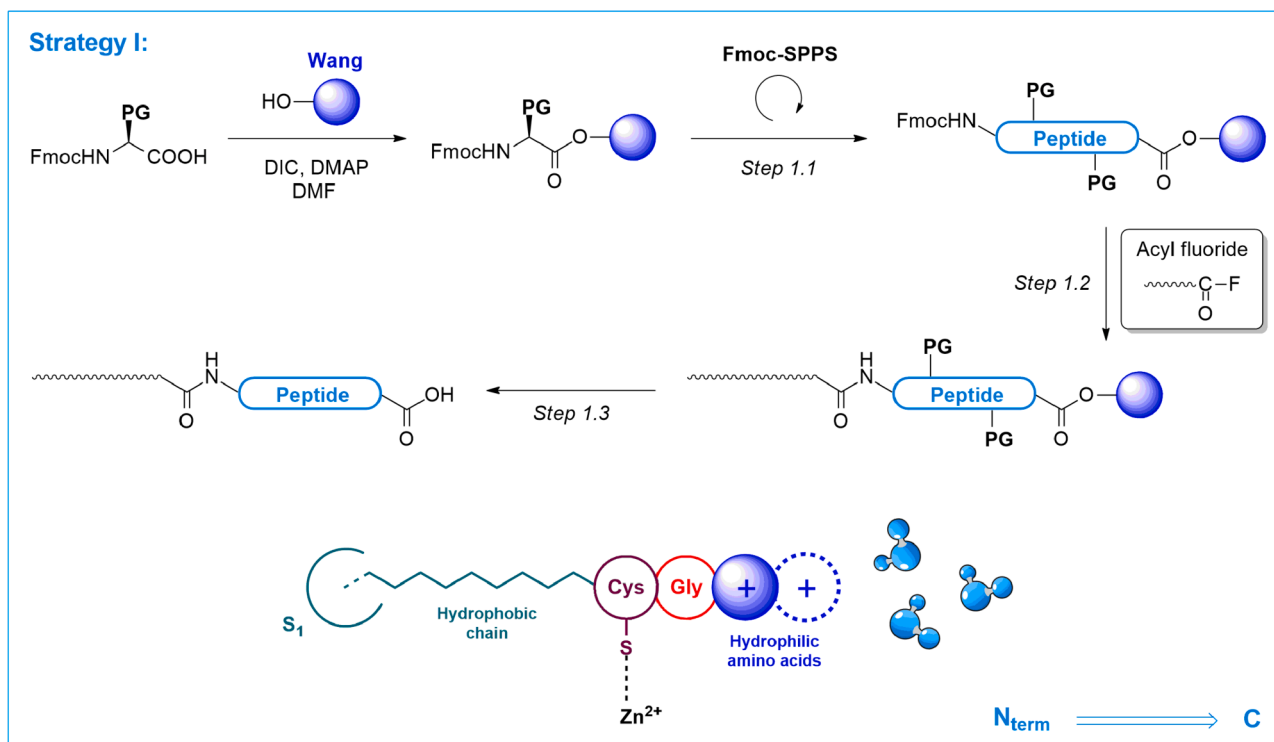
Figure 1. Synthetic strategies applied for the synthesis of the peptide-based inhibitors for MMPs. **Strategy I:** (1.1) Standard Fmoc-SPPS synthesis with Wang resin. (1.2) Fmoc deprotection; addition of acyl fluoride and DIPEA. (1.3) Standard TFA cleavage. **Strategy II:** (2.1) Standard Fmoc-SPPS synthesis with Rink resin. (2.2) Allyl ester deprotection with Pd(PPh$_3$)$_4$ and PhSiH$_3$; activation of the carboxyl group with PyBOP; addition of the alkyl amine. (2.3) Fmoc deprotection; possible addition of acetic anhydride and DIPEA; TFA cleavage.
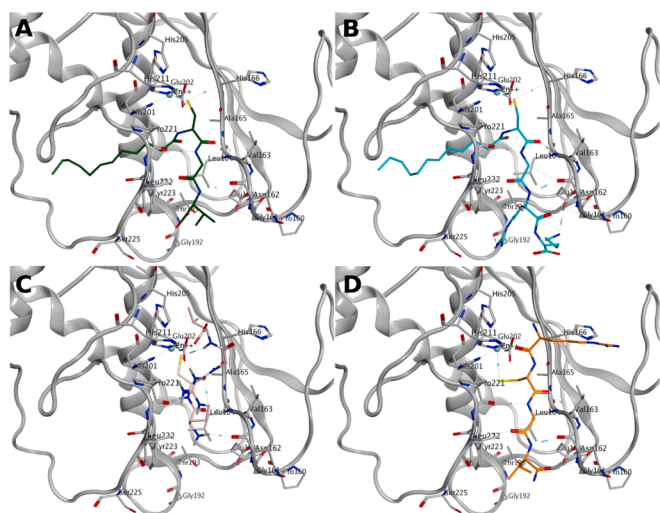
Figure 2. A) Model of the complex between MMP3 (grey) and the modified peptide dodecyl-CGV (dark green). **B)** Model of the complex between MMP3 (grey) and the modified peptide e(I) (cyan). **C).** Model of the complex between MMP3 (grey) and the peptide i(II) (pink) in the 'proenzyme-like' conformation. **D).** Model of the complex between MMP3 (grey) and the peptide i(II) (orange) in the 'RO-26–2812-like' conformation. The enzyme structure (taken from the X-ray structure 1C3I) is represented by a grey ribbon, and the residues within 4.5 Å of the peptide scaffold are represented by sticks. (For interpretation of the references to colour in this figure legend, the reader is referred to the web version of this article.)

the samples were tested in four replicates.

2.6. Collagen release assay of bovine cartilage explants

Normal hyaline cartilage was harvested from the proximal femoral condyles of skeletally mature bovine stifles obtained from a local butchery at maximum 48 h after slaughter. The harvest site did not show any sign of cartilage degradation or swelling upon visual inspection. Full-depth cartilage biopsy samples (Ø = 3 mm) were obtained by means of standard skin biopsy punches (Kay Medical, Italy).

Each cartilage biopsy sample was weighed (mean 16 mg ± 4 mg), placed in a single well of a 48-well plate (Sarstedt, Inc. Germany) and washed 3 times using PBS 1X (Euroclone, Italy) with penicillin/streptomycin solution 1X and amphotericin B 2.5 μg/mL (Life Technologies, Italy). The biopsy samples were then incubated in 500 μL of DMEM/F-12 (Life Technologies, Italy) containing 2.5% FBS (Life Technologies, Italy), 50 μg/mL ascorbic acid (Sigma-Aldrich, Italy), and penicillin/streptomycin solution 1X and amphotericin B 2.5 μg/mL for 24 h under standard culture conditions. After incubation, the biopsy samples were separated into six groups of three replicates each and cultured under the following conditions: (1) in DMEM/F-12 containing 2.5% FBS (CTRL); (2) medium containing IL-1β 10 ng/mL (Life Technologies, Italy) and OSM 10 ng/mL (OriGene, Italy); (3) MMPI: e(I), 93 μM; (4) MMPI: e(I), 3 μM; (5) MMPI: l(II), 127 μM; and (6) MMPI: l(II), 6 μM. All of the MMPI samples tested were previously sterilized by filtration with 0.2 μm filters. The biopsy samples were incubated under standard culture conditions for 3 weeks, with the medium renewed every 7 days. After 21 days, the medium was collected and assayed for soluble collagen content (Sircol Collagen Assay, Biocolor, UK).

2.7. Nile red staining

Nile red was dissolved in acetone to obtain a solution at a concentration of 0.2 mg/mL. Two solutions of peptide e(I) were prepared at 9 mg/mL and 4 mg/mL in PBS at pH = 7. The latter was diluted in PBS until the desired concentrations were reached (2, 1, 0.5, 0.25, 0.125,

0.063, and 0.031 mg/mL). 10 μL of Nile red in acetone were added to1 mL of each solution of peptide e(I) and, as a control, to 1 mL of PBS (final concentration of Nile red equal to 0.02 mg/mL). Each mixture was sonicated for 20 min. After sonication, the solutions were poured into to a 96-well plate (in double), and the Nile red fluorescence was measured (Ex/Em = 510/600 nm). The total volume in each well was 100 μL. The results are reported in Figure 5.

2.8. TEM analysis of peptide e(I) solution

A solution of peptide e(I) at 0.2 mg/mL in PBS (pH = 7) was prepared and then diluted to a final concentration of 0.02 mg/mL in water. 25 μL of this solution was placed on a 400 mesh holey film grid; after staining with 1% uranyl acetate, the sample was analysed with a Tecnai G^2 (FEI) transmission electron microscope operating at 100 kV. Images (Fig. 5) were captured with a Veleta (Olympus Soft Imaging System) digital camera.

2.9. Statistical analysis

The statistical analysis reported for the 'In vitro model of inflammatory arthritis' dataset (Fig. 4) was performed using GraphPad Prism 5.0, applying one-way analysis of variance with Tukey's post hoc analysis; p < 0.05 was considered significant.

3. Results and discussion

3.1. Design, synthesis and potency evaluation of two series of MMP3 inhibitors

The aim of this work is to design a new class of MMP3 inhibitors based on a small peptide sequence, namely, CGV, which is critical for the interaction of the inhibitor with the MMP3 catalytic site. The small peptide was previously described by Hanglow et al.[17], who selected a sequence of three amino acids, CGV, from the structure of the MMP3 pro-domain, because it was pivotal for MMP inhibition activity. In a different study, Steele et al.[18] described a peptide-based MMP3 inhibitor (RO-26–2812) developed from the same three amino acid sequence but chemically modified at the N-terminus with a biphenyl moiety (biphenyl-CGV-OMe). The availability of an X-ray crystal structure of the RO-26–2812-MMP3 complex (PDB code: 1C3I[18]) provided insights
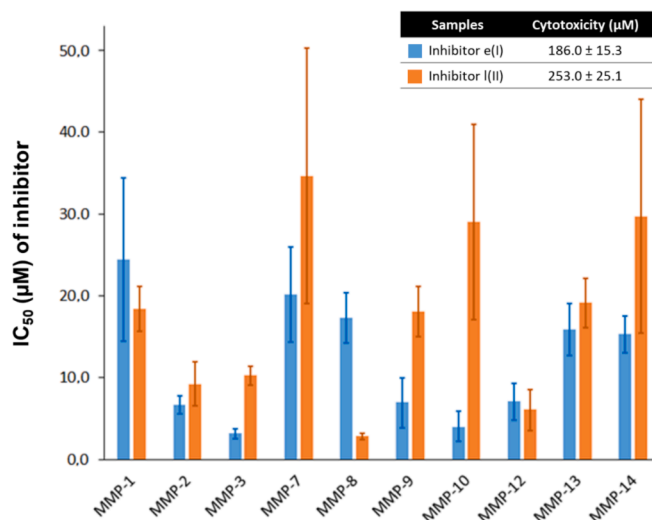

Figure 3. IC$_{50}$ ± SD of two MMPIs: e(I) and I(II) towards the catalytic subunit of ten different human MMPs. The table above shows the cytotoxicity ± SD of the tested compounds (MMPIs: e(I) and l(II)) on BALB/3T3 clone A31 mouse fibroblasts.
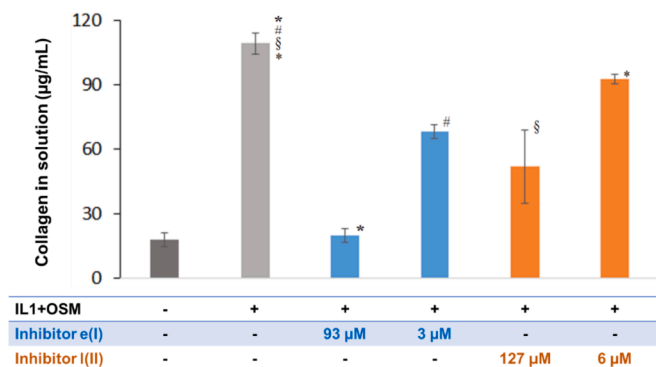
Figure 4. *In vitro* model of inflammatory osteoarthritis. Significant difference *; #; §; * (p < 0.05; n = 4).

into the binding mode of the inhibitor at the enzyme active site: the inhibitor Cys interacts through hydrogen bonds with MMP3 Leu164, the inhibitor Gly interacts with MMP3 Pro221 and Tyr223, and the inhibitor Val interacts with MMP3 Asn162. Moreover, the inhibitor Cys participates to the coordination of the catalytic Zn^{2+} ion through its side chain, while the *N*-terminal biphenyl substituent inserts into the enzyme S1′ hydrophobic cleft. Unexpectedly, the pro-domain CGV sequence (Cys75-Val77) occupies the active site of the pro-enzyme (PDB code: 1SLM;[23]) in an orientation opposite to that of RO-26–2812, with Gly76 interacting with the carbonyl of Ala165, and Cys75 participating to the coordination of the catalytic Zn^{2+} ion through its side chain and interacting with the carbonyl of Pro221. Val77 of the pro-domain CGV sequence is not involved in any interaction with the catalytic site, but a residue preceding the CGV sequence, specifically Arg74, interacts with Leu164 and Asn162.

The availability of these MMP3 crystallographic structures enabled a structure-based approach to design a series of new potential MMP3Is, referred to as Series I. In addition, an empirical strategy was employed to investigate another series of compounds, Series II. For each series, a specific Fmoc-based SPPS procedure was developed (Fig. 1) with two aims: (1) to combine the peptide with an alkyl chain able to block the additional S1′ pocket of the MMP, as observed in the case of HYADD4®; and (2) to increase water solubility by introducing polar amino acids to obtain MMPIs suitable for intra-articular administration.

For Series I of potential MMPIs, the CGV peptide was assumed to bind the enzyme in the same conformation as in the crystallographic pose of RO-26–2812. The CGV portion of RO-26–2812 was in fact stabilized by a pattern of hydrogen bonds with the enzyme, that were lacking in the pro-enzyme conformation. Moreover, the position of the *N*-terminal biphenyl moiety inside the enzyme S1′ pocket straightforwardly suggested the CGV *N*-terminus as a point of attachment for the HYADD4®-like alkyl chain. For this reason, a chemical modification at the *N*-terminus of the CGV peptide with a dodecylamide moiety was considered. The structural interactions between the dodecyl-CGV peptide and the crystal structure of MMP3 were evaluated *in silico*: the compound was built in place on the RO-26–2812 structure and then subjected to minimization. The peptide-enzyme hydrogen bond network described for RO-26–2812 was maintained (Fig. 2, panel A), and the alkyl chain fit into the additional S1′ pocket, with computed electrostatic and van der Waals interaction energies of −150.7 kcal/mol and −30.6 kcal/mol, respectively. Pursuing the aim of increasing the dodecyl-CGV compound solubility, some modifications were suggested on the basis of the compound supposed binding mode. The side chain of the C-terminal Val is not involved in any interaction with the enzyme and is exposed to the solvent, implying that the hydrophobic character of the residue might not be essential for the stabilization of the complex. For this reason, the substitution of Val with a more polar residue, in particular with Arg, was suggested, providing compound a(I). This mutation enhanced the computed electrostatic energy interaction from −150.7 kcal/mol to

−166.8 kcal/mol through the addition of a hydrogen bond between the carbonyl of MMP3 Gly192 residue and the side chain of the peptide Arg.

The dodecylamide (a(I), Table 1) and the octylamide (d(I)) derivatives were chemically synthetized via the SPPS procedure (Fig. 1, Strategy I) and evaluated by a specific MMP3 activity assay. The IC_{50} values of a(I) and d(I) were 7.0 μM and 4.4 μM, respectively, which are both two orders of magnitude lower than those of the nonderivatized peptide (b(I), IC_{50}: 850 μM), highlighting the positive contribution of the alkyl chain to the improved binding affinity.

Since peptides a(I) and d(I) still presented water insolubility, a further chemical modification was proposed on the basis of *in silico* evaluation: specifically, the addition of Lys to the C-terminal portion of MMPI a(I) (dodecyl-CGRK, e(I)) was suggested. The *in silico* evaluation of the e(I)–MMP3 complex shows that the MMPI maintains the same network of interactions, with the addition of a salt bridge between the peptide Lys and the MMP3 Glu184 (Fig. 2, panel B), with a resulting enhanced electrostatic interaction of −215.0 kcal/mol.

The water solubility of peptide e(I) was increased, and the experimental IC_{50} was improved to 3.2 μM. The acetylated peptide (acetyl-CGRK, f(I)) showed an $IC_{50} > 50$ μM, highlighting the fundamental role of the alkyl chain in its inhibitory activity. The length of the alkyl chain was also considered: a variation of the alkyl moiety from 8 to 12 carbons (dodecyl-CGR, a(I) and octyl-CGR, d(I) MMPIs, respectively) negligibly affects the inhibition potency (IC_{50} equal to 7.0 and 4.4 μM, respectively), while an 18-carbon chain (oleyl-CGR, g(I)) decreases the inhibition activity ($IC_{50} > 50$ μM), probably due to the low solubility of the MMPI.

The Series I results suggest that the mutation and addition of positively charged residues at the C-terminal portion of the peptide increase the binding affinity of MMPI for MMP3. Remarkably, an Arg residue precedes the CGV sequence in the pro-domain, and an improved binding affinity is reported for the Ac-RCGV peptide compared to the Ac-CGV peptide[17]. For this reason, the RCGV sequence was employed as a starting point for the second series of compounds (Series II).

The RCGV peptide may hypothetically bind the enzyme in the same conformation it adopts in the pro-enzyme X-ray structure[23]: in this first structural model of the complex the peptide Val is not engaged in any interaction with the enzyme (Fig. 2, panel C). A RO-26–2812-like conformation can also be assumed by the RCGV peptide, preserving the already described pattern of interactions, but a rotation of Cys is required to enable the accommodation of the *N*-terminal Arg to the active site. In this conformation, the Cys side chain points towards the S1′ pocket and the *N*-terminal Arg participates to Zn^{2+} coordination through the carbonyl of the backbone (Fig. 2, panel D). The peptide RCGV-NH₂, i(II) and its *N*-terminal acetylated version (Ac-RCGV-NH₂, l (II)) were synthesized, and, according to the experimental data, the IC_{50} of peptide l(II) (10.2 μM) is more than one order of magnitude lower than that of the free form (i(II), 172.8 μM). The model that better explains the fundamental behaviour of the *N*-terminal acetylation is the RO-26–2812-like conformation, where the peptide *N*-terminus is positioned close to the Zn^{2+} ion (Fig. 2, panel D). In this case, the proximity of the positive ion and the protonated *N*-terminus of the peptide would disfavour binding, with a consequent improvement upon *N*-terminal acetylation.

However, neither the pro-enzyme-like model nor the RO-26–2812-like one suggest a valuable attachment point for the alkyl chain: in both cases the side chain of the Cys faces the S1′ pocket, and a derivatization at this level to engage S1′ pocket would prevent the coordination of Zn^{2+} by Cys. Given the lack of a structure-based rational suggestion, an empirical approach was thus adopted, with the idea of modifying the most hydrophobic residue of the RCGV tetrapeptide, i.e., the C-terminal Val. This amino acid was mutated into Asp and chemically derivatized at the side chain with an octylamide moiety. This MMPI (CGD(-octyl), g (II)) was synthetized via the SPPS procedure (Fig. 1, Strategy II) but did not show interesting results, with an $IC_{50} > 200$ μM (and 61.4 μM for the *N*-terminal acetylated analogue, g(II)). A further attempt was made by

Table 1

Series I and **Series II** of peptide-based MMPIs. Experimentally measured solubility and inhibition potency towards MMP3.

Name (Series)	Sequence	R′	Water solubility (at 1 mg/mL)	IC$_{50}$± SD $vs.$ MMP3(μM)
a (I)	R′-CGR	CH$_3$(CH$_2$)$_{10}$CO-	N	7.0±1.3
b (I)	R′-CGR	CH$_3$CO-	N	850.1±35.2
c (I)	R′-CGR	CH$_3$(CH$_2$)$_7$CH=CH(CH$_2$)$_7$CO-	N	>50
d (I)	R′-CGR	CH$_3$(CH$_2$)$_6$CO-	N	4.4±0.8
e (I)	**R′-CGRK**	**CH$_3$(CH$_2$)$_{10}$CO-**	**Y**	**3.2±0.6**
f (I)	R′-CGRK	CH$_3$CO-	Y	>50
g (II)	RCGD(-R′)-NH$_2$	-NH(CH$_2$)$_7$CH$_3$	N	>200
h (II)	Ac-RCGD(-R′)-NH$_2$	-NH(CH$_2$)$_7$CH$_3$	Y	61.4±7.1
i (II)	RCGV-NH$_2$	/	Y	172.8±5.2
l (II)	**Ac-RCGV-NH$_2$**	**/**	**Y**	**10.2±1.1**
m (II)	Ac-RCG-NH$_2$	/	Y	95.3±6.5
n (II)	Ac-RCG-R′-NH$_2$	-Nle-	Y	79.5±7.3

substituting Val with Nle (n(II)), but similarly, in this case, the activity of l(II) was not improved, with an IC$_{50}$ of 79.5 μM. This behaviour can be explained by both models, where Val is positioned far from the entrance to the S1′ pocket (highlighted by a green circle in Fig. 2, panel C).

In summary, e(I) and l(II) MMPIs were selected as lead compounds of the two series on the basis of their good inhibitory activity and water solubility, and they were subjected to further studies.

3.2. Selectivity of the selected MMPIs: e(I) and l(II) vs. Human MMPs and cytotoxicity assessment

In this study, the two selected peptide-based MMPIs were screened *in vitro* at different concentrations against 10 different human MMPs; PBS buffer was used as a negative control. As reported in Fig. 3, both MMPIs e(I) and l(II) showed a broad spectrum of inhibition against almost all MMPs, with the highest inhibition potency against MMP8, MMP12, MMP2 and MMP3 for l(II) and towards MMP2, MMP3, MMP9, MMP10 and MMP12 for e(I), with an IC$_{50} \leq 10$ μM for both MMPIs.

The cytotoxicity of the e(I) and l(II) MMPIs was also evaluated (according to ISO 10993–5) in a mouse fibroblast cell line (BALB/3T3). The test was performed by exposing the cells to increasing concentrations of e(I) or l(II). The results of the cytotoxicity assay are summarized in the table in Fig. 3: both MMPIs did not show cytotoxicity at any of the doses effective in the MMP activity assay.

3.3. Efficacy of MMPIs: e(I) and l(II) in an in vitro model of inflammatory OA

To evaluate the biological activity of the selected peptide-based MMPIs, a cartilage explant culture model was established. The cartilage explants harvested from bovine condyles were treated with inflammatory cytokines (OSM and IL-1β) to elicit an inflammatory response. During inflammation, cartilage tissue secretes MMPs in the extracellular environment, inducing cartilage degradation[24] The cartilage samples were separately treated with e(I) or l(II) MMPIs at two different concentrations. After 21 days of incubation, the concentration of the collagen released into the medium was quantified by a specific assay. The results are summarized in Fig. 4. As expected, the cartilage explants exposed to pro-inflammatory cytokines (positive control) showed significant collagen release into the culture medium compared to the untreated explants (negative control). The treatment of the inflamed cartilage explants with both MMPIs significantly reduced the release of collagen fragments in solution compared to the level released by the inflamed explant (positive control). Moreover, MMPI e(I), at a concentration of 93 μM, reduced the release of collagen fragments in solution to the level of the untreated control. Based on these results, it is

likely that MMPI e(I) plays a role in reversing the inflammatory outcome in this *ex vivo* model of OA. Moreover, alkyl derivatization of the peptide backbone in the e(I) MMPI gives an amphiphilic structure that can potentially increase the bioavailability and thus the efficacy of the MMPI.[25]

3.4. Self-assembly of the amphiphilic MMPI: e(I)

Peptide amphiphiles are a class of molecules that combine the structural features of amphiphilic surfactants with the functions of bioactive peptides, and they are known to assemble into a variety of nanostructures. In e(I), the amphiphilic structure is constituted by hydrophilic amino acid sequences coupled to hydrophobic alkyl chains; potentially, the self-assembly of this MMPI in nanostructures would increase the residence time and thus the efficacy of the MMPI.[25] The ability and relative concentration of e(I) to produce amphiphilic nanostructures (like micelles) has been studied by Nile red staining.

Nile red is a solvatochromic fluorophore that can be used to detect the polarity of the medium in which it is solvated. It is nearly insoluble in water but is very soluble and shows high fluorescence in nonpolar organic solvents; consequently, the incorporation of the dye into amphiphile nanostructures in an aqueous medium increases the fluorescence at 600 nm.[26] The formulation of e(I) in PBS was characterized by increasing concentrations of the peptide mixed with a fixed concentration of Nile red, whose fluorescence emission was measured at 600 nm. The results are summarized in Fig. 5A: for a concentration smaller than 0.2 mg/mL, the fluorescence intensity is constant or increases slightly, whereas at concentrations>0.2 mg/mL, the fluorescence intensity increases sharply, as peptide e(I) self-assembles into nanostructures and captures the dye molecules. The interpolation of these two datasets produces a critical micelle concentration (CMC) value equal to 0.207 mg/mL.

Finally, TEM images of peptide e(I) showed the presence of spherical aggregates with diameters of approximately 50 nm (Fig. 5B), compatible with amphiphilic nanostructures as micelles of different shapes such as spherical, ellipsoidal or rod-like.

4. Conclusion

In this study, a new class of MMPIs was developed through interactive cycles of design, synthesis and screening followed by computational evaluation and optimization. This class of MMP3Is is based on a small peptide backbone (CGV) chemically derivatized with an alkyl chain, in which the CGV sequence is critical for the interaction with the MMP3 catalytic site, while the alkyl side chain is able to occupy the additional S1′ pocket of the MMP. Two MMP3Is, e(I) and l(II), were selected due to
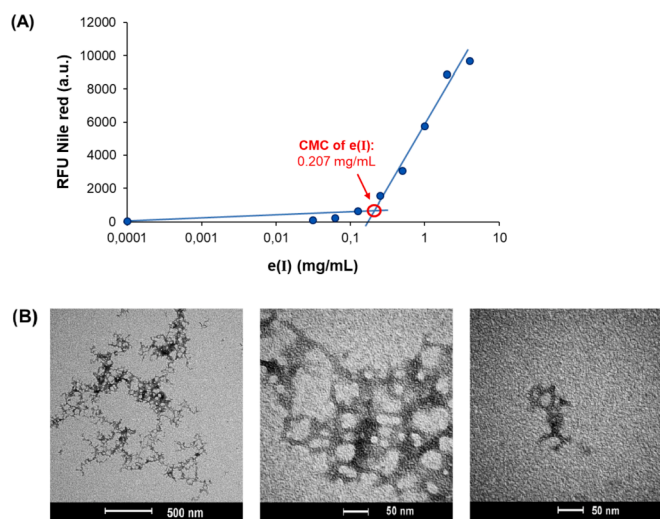
Figure 5. **(A)** Correlation between the fluorescence of Nile red and the concentration of peptide **e(I)** (fixed concentration of Nile red). The red-circled interpolation point shows the CMC for peptide e(I). **(B)** TEM images of peptide **e(I)** solution. (For interpretation of the references to colour in this figure legend, the reader is referred to the web version of this article.)

their good inhibitory activity (3.2 and 10.2 μM, respectively) and water solubility. e(I) is the result of a structure-based drug design approach grounded in the experimental binding mode of the known inhibitor RO-26–2812 (Series I). l(II) was part of an empirical investigation involving the modification of the sequence RCGV, the portion of the pro-domain that binds the enzyme catalytic site (Series II). Both MMPIs showed a wide range of inhibitory effects against almost all the MMPs tested and did not exhibit cytotoxicity at any of the effective doses. In an *in vitro* model of inflammatory OA, MMPI e(I) was the most active, and the concentration of 93 μM MMPI e(I) reversed the inflammatory outcome. Moreover, based on TEM and the Nile red staining analysis, the amphiphilic structure of e(I) MMPI produces a stable micellar formulation at concentrations higher than 0.2 mg/mL in water. Based on these findings, MMPI e(I) can be considered a good candidate for the intra-articular treatment of OA, and the micellar formulation of this peptide in an aqueous buffer can potentially increase the bioavailability and thus the efficacy of the MMPIs.

Declaration of Competing Interest

The authors declare the following financial interests/personal relationships which may be considered as potential competing interests:

At the time of the study: Cristian Guarise, Martina Tessari, Mauro Pavan, Carlo Barbera, Riccardo Beninatto and Devis Galesso were full-time employees of Fidia Farmaceutici SpA.

Davide Ceradini was in a thesis internship at Fidia Farmaceutici SpA.

The activities of Stefano Moro and Veronica Salmaso were paid by Fidia Farmaceutici SpA.

Acknowledgements

Appendix A. Supplementary data

Supplementary data to this article can be found online at https://doi. org/10.1016/j.bmc.2021.116132.

References

1 Vandenbroucke RE, Libert C. Is There New Hope for Therapeutic Matrix Metalloproteinase Inhibition? *Nat Rev Drug Discov*. 2014;13:904–927. https://doi. org/10.1038/nrd4390.
2 Page-McCaw A, Ewald AJ, Werb Z. Matrix Metalloproteinases and the Regulation of Tissue Remodelling. *Nat Rev Mol Cell Biol*. 2007;8:221–233. https://doi.org/ 10.1038/nrm2125.
3 Gaffney J, Solomonov I, Zehorai E, Sagi I. Multilevel Regulation of Matrix Metalloproteinases in Tissue Homeostasis Indicates Their Molecular Specificity in Vivo. *Matrix Biol*. 2015;44–46:191–199. https://doi.org/10.1016/j. matbio.2015.01.012.
4 Renckens R, Roelofs JJTH, Florquin S, et al. Matrix Metalloproteinase-9 Deficiency Impairs Host Defense against Abdominal Sepsis. *J Immunol*. 2006;176:3735–3741. https://doi.org/10.4049/jimmunol.176.6.3735.
5 Caley MP, Martins VLC, O'Toole EA. Metalloproteinases and Wound Healing. *Adv Wound Care*. 2015;4:225–234. https://doi.org/10.1089/wound.2014.0581.
6 Konttinen YT, Ainola M, Valleala H, et al. Analysis of 16 Different Matrix Metalloproteinases (MMP-1 to MMP-20) in the Synovial Membrane: Different Profiles in Trauma and Rheumatoid Arthritis. *Ann Rheum Dis*. 1999;58:691–697. https://doi.org/10.1136/ard.58.11.691.
7 Martel-Pelletier J, Welsch DJ, Pelletier J-P. Metalloproteases and Inhibitors in Arthritic Diseases. *Best Pract Res Clin Rheumatol*. 2001;15:805–829. https://doi.org/ 10.1053/berh.2001.0195.
8 Mirastschijski U, Impola U, Jahkola T, Karlsmark T, Ågren MS, Saarialho-Kere U. Ectopic Localization of Matrix Metalloproteinase-9 in Chronic Cutaneous Wounds. *Hum Pathol*. 2002;33:355–364. https://doi.org/10.1053/hupa.2002.32221.
9 Rivera S, García-González L, Khrestchatisky M, Baranger K. Metalloproteinases and Their Tissue Inhibitors in Alzheimer's Disease and Other Neurodegenerative Disorders. *Cell Mol Life Sci*. 2019;76:3167–3191. https://doi.org/10.1007/s00018-019-03178-2.
10 Rakash S. Role of Proteases in Cancer: A Review. *Biotechnol Mol Biol Rev*. 2012;7: 90–101. https://doi.org/10.5897/BMBR11.027.
11 Peterson JT. Matrix Metalloproteinase Inhibitor Development and the Remodeling of Drug Discovery. *Heart Fail Rev*. 2004;9:63–79. https://doi.org/10.1023/B: HREV.0000011395.11179.af.
12 Burrage PS, Brinckerhoff CE. Molecular Targets in Osteoarthritis: Metalloproteinases and Their Inhibitors. *Curr Drug Targets*. 2007;8:293–303. https://doi.org/10.2174/ 138945007779940098.
13 Fields GB. The Rebirth of Matrix Metalloproteinase Inhibitors: Moving Beyond the Dogma. *Cells*. 2019;8:1–24. https://doi.org/10.3390/cells8090984.
14 Li NG, Shi ZH, Tang YP, Duan JA. Selective Matrix Metalloproteinase Inhibitors for Cancer. *Curr Med Chem*. 2009;16:3805–3827. https://doi.org/10.2174/ 092986709789178037.
15 Visse R, Nagase H. Matrix Metalloproteinases and Tissue Inhibitors of Metalloproteinases: Structure, Function, and Biochemistry. *Circ Res*. 2003;92: 827–839. https://doi.org/10.1161/01.RES.0000070112.80711.3D.
16 Guarise C, Pavan M, Galesso D, et al. *Osteoarthritis and Cartilage*. 2018;26:S286–S287. https://doi.org/10.1016/j.joca.2018.02.577.
17 Hanglow AC, Lugo A, Walsky R, et al. Peptides Based on the Conserved Prodomain Sequence of Matrix Metalloproteinases Inhibit Human Stromelysin and Collagenase. *Agents Actions*. 1993;39:C148–C150. https://doi.org/10.1007/BF01972749.
18 Steele DL, El-Kabbani O, Dunten P, et al. Expression, Characterization and Structure Determination of an Active Site Mutant (Glu202–Gln) of Mini-Stromelysin-1. *Protein Eng Des Sel*. 2000;13:397–405. https://doi.org/10.1093/protein/13.6.397.
19 Labute P. Protonate3D: Assignment of ionization states and hydrogen coordinates to macromolecular structures. *Proteins*. 2009;75:187–205. https://doi.org/10.1002/ prot.22234.
20 Molecular Operating Environment (MOE), 2016.08; Chemical Computing Group ULC, 1010 Sherbooke St. West, Suite #910, Montreal, QC, Canada, H3A 2R7, 2017.
21 Jones G, Willett P, Glen RC, Leach AR, Taylor R. Development and validation of a genetic algorithm for flexible docking. *J Mol Biol*. 1997;267:727–748. https://doi. org/10.1006/jmbi.1996.0897.
22 Guarise C, Barbera C, Pavan M, Pluda S, Celestre M, Galesso D. Dopamine-functionalized sulphated hyaluronic acid as a titanium implant coating enhances biofilm prevention and promotes osseointegration. *Biofouling*. 2018;14:719–730. https://doi.org/10.1080/08927014.2018.1491555.
23 Becker JW, Marcy AI, Rokosz LL, et al. Stromelysin-1: Three-dimensional structure of the inhibited catalytic domain and of the C-truncated proenzyme. *Protein Sci*. 1995;4: 1966–1976. https://doi.org/10.1002/pro.5560041002.
24 Goldring MB. The role of the chondrocyte in osteoarthritis. *Arthritis Rheum*. 2000;43: 1916–1926. https://doi.org/10.1002/1529-0131(200009)43:9<1916::AID-ANR2>3.0.CO;2-I.
25 Cui H, Webber MJ, Stupp SI. Self-assembly of peptide amphiphiles: From molecules to nanostructures to biomaterials. *Pept Sci*. 2010;94:1–18. https://doi.org/10.1002/ bip.2132.
26 Carmichael AJ, Seddon KR. Polarity study of some 1-alkyl-3-methylimidazolium ambient-temperature ionic liquids with the solvatochromic dye, Nile Red. *J Phys Org Chem*. 2000;13:591–595. https://doi.org/10.1002/1099-1395(200010)13:10<591: AID-POC305>3.0.CO;2-2.